Smart Wireless Headphone for Cardiovascular and Stress Monitoring

Bruno M. G. Rosa
Imperial College London
South Kensington Campus
London SW7 2AZ, UK
Email: b.gil-rosa@imperial.ac.uk

Guang Z. Yang
Imperial College London
South Kensington Campus
London SW7 2AZ, UK
Email: g.z.yang@imperial.ac.uk

***Abstract*—Wearable technology has become ubiquitous in recent years due to the miniaturization of circuit electronics and advances in smart materials that can conform to the requirements posed by the human body, behaviour and experience. Sensors of this type are found attached almost to every body segment, capable of delivering signals even in harsh activity scenarios. The reliability and relevance of the physiological data retrieved by *wearables* have yet to surpass the conventional technologies in the healthcare system today. In this paper we present a small device incorporated inside an headphone set that continuously monitors the ECG, impedance and acceleration of the head. As opposed to most biometric sensors, ECG measurement relies on non-optical methods by capturing the electrical potential around the ear in both sides of the head, whereas impedance monitoring involves AC stimulation instead of DC, the latter commonly involved in skin galvanic response estimation. Signal processing of impedance parameters is performed *in situ* using a fast variant of the Discrete Fourier Transform in order to save computational resources and power expenditure from a microcontroller equipped with Bluetooth Low Energy. Applications that can benefit from this device include cardiovascular and stress level assessment of individuals for whom an *hearable* is a requirement for work or leisure.**

I. Introduction

Wearable biometric technology is an open field of research in the academic community and healthcare organizations that aim to produce tiny body sensors with telemetric capabilities and minimal power consumption. Digital signal processing can be performed to some extent at the sensor level to complement the physiological measurements with context awareness. These devices include glucose meters, biopotential monitors, body motion detectors and odour sensors [1], [2], [3]. The heart rate monitor embodied as a wrist band or watch is the most abundant one that counts the heart beat *via* the detected peaks in the artery pulse when excited by light. Examples are the Apple Watch, Garmin Forerunner and Polar M600, to name a few.

Thus far, several technologies have also been proposed to track the response of the autonomous nervous system (ANS) during stressful situation. Malfunctioning of the ANS can lead to diseases such as cardiovascular, gastrointestinal, neuropsychiatric, motor dysfunction and pain [4], [5]. Typical signals for stress assessment include the galvanic skin response (GSR), skin temperature and heart rate variability [4], [6]. While the latter ones can be acquired by almost all the wearable devices in the market today, for GSR it is more subtle since it requires the stimulation of the tissue under analysis and record its conductance. It has been shown that the increase on the level of sweat due to stress produces a signal rise in GSR that can be detected using proper electronics [7]. Based on this principle, some technologies have been developed such as Neumitra that measures proxies for stress and/or excitement and Affectiva to establish a physiological measure for pain. However, these technologies only explore the DC regime of stimulation excluding the AC counterpart involved in important cellular processes as given by Schawn's model for bioimpedance [8], [9].

Much of the wearable devices today are designed to be conformal to the body segment they target in order to minimize discomfort as possible and much potential can be offered by the earlobes. In fact, the unique anatomy of the ear helps the so-called *hearable* devices to conform to the natural contour of the head while allowing direct contact to the skin around the earlobes, potential areas for recording the ECG, EEG, GSR and artery pulse. To that end, smart headphones

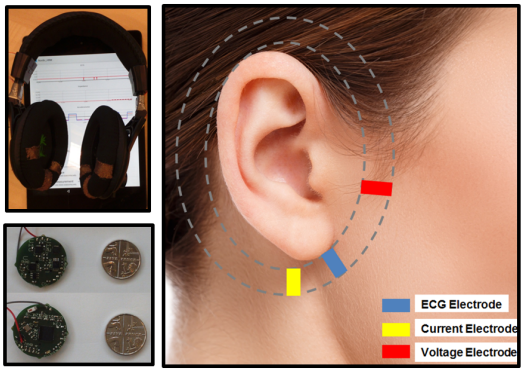

Fig. 1. Smart wireless headphone set: external aspect with recording tablet, embedded electronics for the device (top and bottom layers) and electrode placement around the right ear. Electrodes made of conductive fabric are in contact with the skin between the internal and external borders of the ear-cup (dashed lines) in both sides of the head. Wires connect the electrodes from the left ear-cup to the right one where the device is located, allowing bipolar ECG measurements and impedance recording of the head segment.

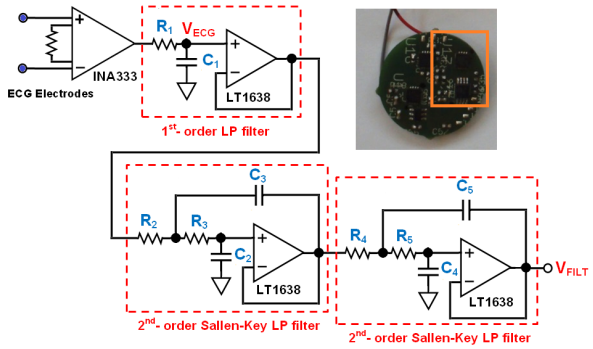

Fig. 2. ECG acquisition channel with an amplification stage followed by a 5^{th}-order Butterworth low-pass filter. The filter is itself a combination of a 1^{st}-order filter with two 2^{nd}-order Sallen-Key low-pass filters. The inlet highlights the dedicated electronics in the circuit board of the device.

like the Jabra Sport Pulse, Bose SoundSport Pulse or Bragi Dash track heart rate through optical readings as well as other fitness parameters at rest or during exercise to provide augmented experience to the end user.

In this paper we present a smart device for cardiovascular and stress assessment based on a different measuring approach that can be used by musicians and athletes alike, or in any stressful job where the need to wear headphones is mandatory like emergency first responders or air-plane pilots.

II. Material and Methods

This section describes the electronics involved in the design of the smart device, divided into three modules: ECG acquisition channel, impedance measurement system and communication framework. The latter includes information regarding the embedded accelerometer and signal transmission by means of Bluetooth Low Energy (BLE).

A. ECG acquisition channel

Any biopotential acquisition system requires a low noise instrumentation amplifier with high CMMR to differentially amplify the signal of interest and reject common-mode interferences. Since the ECG is acquired outside the chest, an higher gain of 100 V/V is set for the amplifier - the INA333 from Texas Instruments -, as depicted in Fig. 2. Also, the conductive fabric of the electrodes helps to lower the contact impedance and voltage drift in the acquired signal. An high-order analogue filter is deployed after amplification to sharpen the frequency content of the ECG signal in order to eliminate noise interferences, specially the capacitive coupling between the human body and the 50 Hz power grid signal. Dimensioning of the resistors present on the filter is performed in Eq. 1 by imposing a cut-off frequency, f_{cut}, of 20 Hz and values for the capacitors as C_1 = 4.7 μF, C_2 = 15 nF, C_3 = 33 nF, C_4 = 8.2 nF and C_5 = 100 nF [10].

$$\begin{cases} R_1 = \frac{1}{2\pi f_{cut} C_1} \approx 1.8\ k\Omega \\ R_2 = \frac{a_2 C_3 - \sqrt{a_2^2 C_3^2 - 4 C_2 C_3}}{4\pi f_{cut} C_2 C_3} \approx 190\ k\Omega \quad (a_2 = 1.62) \\ R_3 = \frac{a_2 C_3 + \sqrt{a_2^2 C_3^2 - 4 C_2 C_3}}{4\pi f_{cut} C_2 C_3} \approx 670\ k\Omega \\ R_4 = \frac{a_3 C_5 - \sqrt{a_3^2 C_5^2 - 4 C_4 C_3}}{4\pi f_{cut} C_4 C_3} \approx 190\ k\Omega \quad (a_3 = 0.62) \\ R_5 = \frac{a_3 C_5 + \sqrt{a_3^2 C_5^2 - 4 C_4 C_3}}{4\pi f_{cut} C_4 C_3} \approx 420\ k\Omega \end{cases} \tag{1}$$

The filter output is then digitalized with 10-bit of resolution by the embedded microcontroller - the nRF51822 from Nordic Semiconductors - working at a rate of 140 SPS for ten consecutive seconds, interleaved by the impedance measurement process, as described in the next section.

B. Impedance measurement system

The tetra-polar system is the most standard configuration for impedance measurements which makes use of a pair of current-injecting electrodes to create entry and exit ports for the excitation current to flow and a pair of voltage-sensing electrodes whose positioning determines the segment of the tissue to be measured [11], [12]. Conversion from the voltage signal provided by the microcontroller (MCU) to current is performed by an operation amplifier - the LT1638 from Linear Technology - mounted in a transadmittance configuration. Current is set as the ratio between the voltage at the positive input terminal, V_{EXC}, and resistor R_{SET}, as shown in Fig. 3. For a 2 V signal, a resistor of 47 kΩ is required to set the excitation current to a safe level of 50 μA. Voltage swing in the feedback loop must also be kept within the power supply levels since the total load will multiply by this excitation current. For the present conditions, the maximum load allowed in the loop is 22 kΩ. The calculation of the load value, Z_L, is given as,

$$\frac{1}{Z_L} = \frac{1}{Z_R} + \frac{1}{2Z_C + Z_T} \iff Z_L = \frac{2Z_C + Z_T}{\frac{2Z_C}{Z_R} + \frac{Z_T}{Z_R} + 1} \tag{2}$$

which, by setting $Z_R \gg Z_T$ and $Z_C \to 0$ for a 1 kHz sine-wave, one achieves $Z_L \approx Z_T$. This means that a change in the load is solely due to a variation in the tissue impedance being analysed. The additional capacitors prevent low-level DC currents originating at amplifier level to get into the living tissues, whereas Z_R assures that there is remains a closed

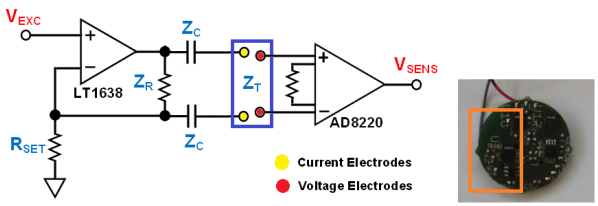

Fig. 3. Circuit involved in tissue impedance measurements (Z_T). V_{EXC} is obtained from a square signal with attenuation of the DC level and higher order harmonics. The inlet shows the area occupied by embedded electronics.

loop for these currents to flow. DC blockage is mandatory since it avoids some physiological impairments for the tissue namely electrolysis and permanent migration of free ions [8].

For signal acquisition, a low-noise instrumentation amplifier - the AD8220 from Analog Devices® - is used with a gain set to 50 V/V that can sense the signal developed across the voltage-sensing electrodes connected to both ear cups. The output of the amplifier is then digitalised with a sample rate of 8 kSPS. The computation of the parameters for impedance - magnitude and phase - is also performed inside the MCU as soon as the required samples are captured - 80 in total - that corresponds to 8 samples *per* 10 consecutive periods of the 1 kHz sinus. The remaining time is spent to process the Discrete Fourier Transform (DFT) after which, the ECG acquisition process can resume again.

DFT computes the frequency transform for both the excitation and sensing channels, V_{EXC} and V_{SENS} (when corrected from gain), respectively, yielding a number of coefficients equal to the length of the samples vector as,

$$X_k = \sum_{n=0}^{N-1} x_n \exp\big(-j2\pi k \frac{n}{N}\big), \quad k = 0, .., N-1 \qquad (3)$$

where x_k is the sample with index k and N the number of samples. Since DFT estimates coefficients up to half the sample rate (4 kHz), by centring the spectrum at the middle of the frequency span, X_{40} will yield the DC level and X_{79} the 4 kHz component minus the resolution step, Δf = 100 Hz. The coefficient for the excitation signal at 1 kHz corresponds to X_{50} and only this coefficient is explicitly calculated by the MCU with real and imaginary components of the form,

$$\begin{cases} \Re\{X_{50}\} = \sum_{n=0}^{79} x_n \cos\big(-j2\pi * 50\frac{n}{N}\big) = D_N.W_{coef}^{real} \\ \Im\{X_{50}\} = \sum_{n=0}^{79} x_n \sin\big(-j2\pi * 50\frac{n}{N}\big) = D_N.W_{coef}^{imag} \end{cases} \qquad (4)$$

with D_N being the vector containing all digital samples and W_{coef}^{real} and W_{coef}^{imag} vectors with the binary codes for the real and imaginary weights, respectively, which are fixed and stored inside the program data of the MCU. The remaining formulae to complete the calculation of the amplitude and phase are given by Eqs. 5 and 6.

$$|Z_T| = R_{SET} \frac{\sqrt{\Re\{X_{50}^{SENS}\}^2 + \Im\{X_{50}^{SENS}\}^2}}{\sqrt{\Re\{X_{50}^{EXC}\}^2 + \Im\{X_{50}^{EXC}\}^2}} \qquad (5)$$

$$\angle Z_T = \arctan\left(\frac{\Im\{X_{50}^{SENS}\} - \Im\{X_{50}^{EXC}\}}{\Re\{X_{50}^{SENS}\} - \Re\{X_{50}^{EXC}\}}\right) \qquad (6)$$

C. Communication framework

A graphical user interface was developed inside Android Studio using the framework dedicated for BLE communication with peripheral devices. The device sends a valid data packet to a remote tablet or phone every 100 millisecond with a payload of 20 bytes. The packet contains either the acquired ECG samples or impedance estimation parameters, together with the data retrieved from a three-axis accelerometer - the MMA7660 from NXP - and an extra byte identifier, so it can distinguish between ECG or impedance measurements. The sample rate set for the accelerometer is 30 SPS with an axis range of ±1.5 g and resolution close to 0.1 g. The information given by the accelerometer serves two purposes: first, voltage excursions produced by motion artifacts can be ruled out from recordings if a sudden movement of the head has occurred; second, movement trembling as a result of some medical impairments can have a correlation in the ECG and/or impedance signals being recorded.

III. Results

Figures 4 and 5 show the performance of the ECG and impedance channels, respectively, to highlight the technical considerations taken in the design of the electronic stages to enhance signal detection and quantification. The attenuation of the 50 Hz component from the ECG signal is of paramount importance so the algorithm that tracks heart beat (bpm) on the remote side does not get stuck with the noise peaks between QRS complexes, whereas the impedance curve is calibrated for the low kΩ range as skin impedance in AC

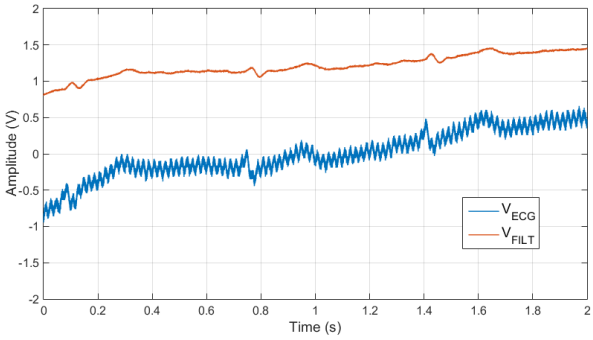

Fig. 4. ECG acquisition channel developed for the smart device with the signals taken at the output of the instrumentation amplifier (V_{ECG}) and 5^{th}-order Butterworth low-pass filter (V_{FILT}). V_{ECG} oscillates between negative and positive values whereas V_{FILT} is DC-biased in order to be within the positive range of the internal ADC.

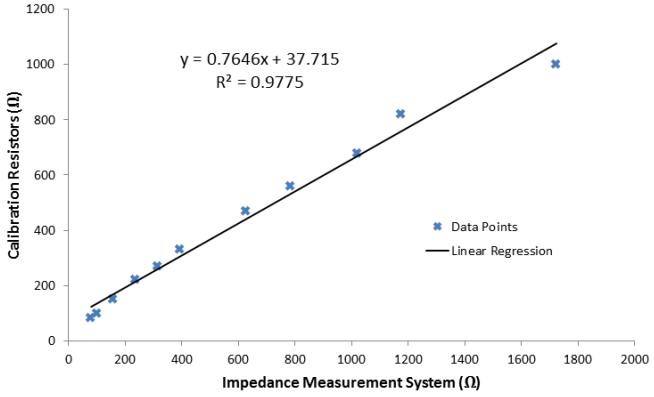

Fig. 5. Calibration curve with estimation parameters for the impedance, as calculated by the device with a 1 kHz sinewave excitation. The current-carrying electrodes are connected to the voltage-sensing ones, converting the tetra-polar configuration into a bipolar measurement involved in the computation of impedance for some calibrated resistors (phase = 180°).

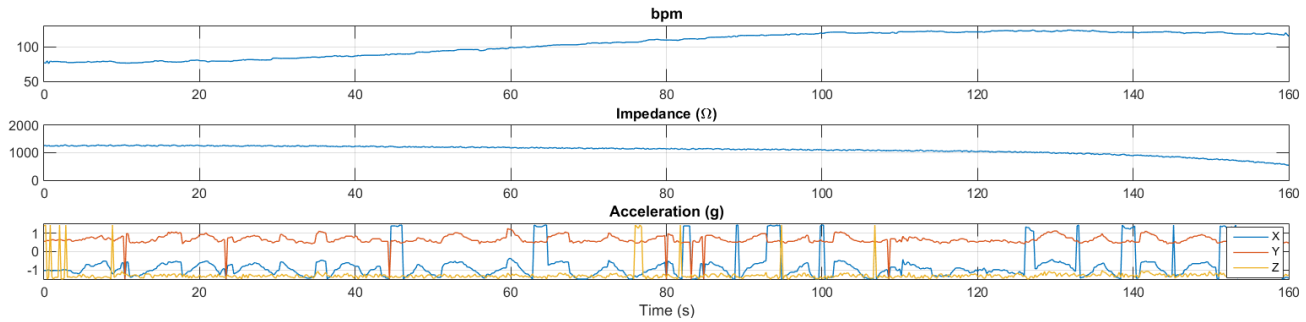

Fig. 6. Extended temporal recording obtained during weight-lifting exercise, exhibiting the tilting of the head in the XY-plane and the continuous decline of the impedance level as sweating starts to occur, whereas the number of heart beats increases.

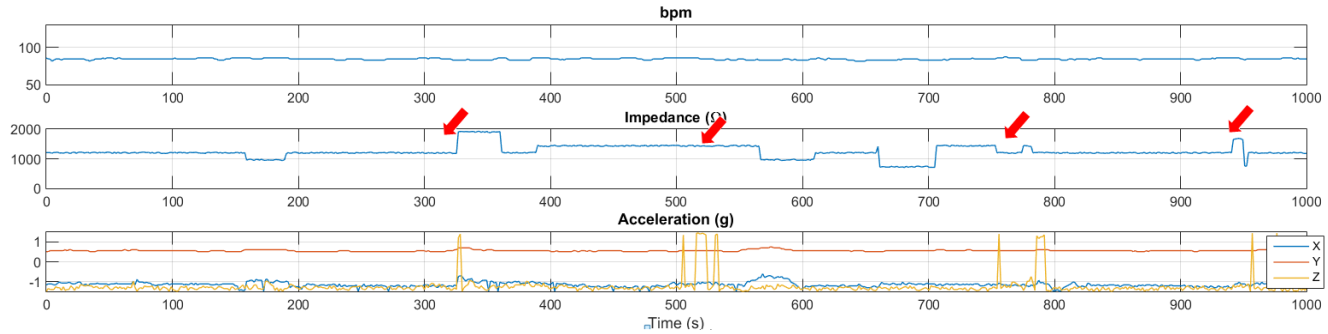

Fig. 7. Extended temporal recording obtained during music listening. The red arrows show the moment of time for a sudden sound level rise to induce surprise on the subject, which responds with an abrupt movement of the head (z-axis) and some evident signal fluctuations on the impedance level.

regime is smaller than DC (10 kΩ to 10 MΩ) [7]. By its turn, Figs. 6 and 7 show recordings for assessment of heart beat, stress level and motion for two situations: exercise (weight-lifting) and listening to music (sudden sound level variation).

IV. Discussion

In summary, we have presented a smart device for cardiovascular and stress level evaluation that records physiological signals around the ears. The bipolar ECG acquisition has forced the use of an headband to provide measurements with some distance between recording sites whereas, for impedance monitoring, a single earpiece could have provided enough information as this type of measurement can be performed for short-length segments, if the current-injecting electrodes enclose the voltage-sensing ones. The advantage of direct skin contacts for biopotential recording over light methods is that the underlying waveform can be truly sampled and transmitted, instead of a set of features extracted from the peaks or valleys in the signal. For cardiovascular diseases this is extremely important since many impairments are identified by the electrical trace only. Nonetheless, the location of the earlobe nearby constitutes a good site for optical pulse oximetry measurements as the skin is thinner, complementing the data provided by the device. Correlation between heart beat, stress and motion needs also to be investigated more deeply to identify the ANS responses, for which, the present paper is just a reasonable contribution.

Acknowledgment

The authors would like to thank to the Engineering and Physical Science Research Council for the financial support under the project grant ”EPSRC EP/L014149/1”.

References

[1] Yang, G. Z., *Body Sensor Networks.* Springer, London, 2006.
[2] Bronzino, J. D. and Peterson, D. R., *The Biomedical Engineering Handbook - Fourth Edition.* CRC Press, 2015.
[3] Fitzpatrick, D., *Implantable Electric Medical Devices.* Elsevier Ltd., Oxford, 2015.
[4] Yoon, S. *et al.*, *A Flexible and Wearable Human Stress Monitoring Patch.* Nature Scientific Reports 6:23468, 2016.
[5] Vahey, R. and becerra, R., *Galvanic Skin Response in Mood Disorders: A Critical Review.* International Journal of Psychology and Psychological Theraphy, vol. 15, no. 2, pp. 275 - 304, 2015.
[6] Vijaya, P. A, and Shivakumar, G., *Galvanic Skin Response: A Physiological Sensor System for Affective Computing.* International Journal of Machine Learning and Computing, vol. 3, no. 1, 2013.
[7] Villarejo, M. V. *et al.*, *A Stress Sensor Based on Galvanic Skin Response (GSR) Controlled by ZigBee.* Sensors, vol. 12, pp. 6075 - 6101, 2012.
[8] Grimnes, S. and Martinsen, O. G., *Bioimpedance and Bioelectricity Basics - Second Edition.* Elsevier Ltd., 2008.
[9] Davalos, R. V. *et al.*, *A Feasibility Study for Electrical Impedance Tomography as a Means to Monitor Tissue Electroporation for Molecular Medicine.* IEEE Transactions on Biomedical Engineering, vol. 49, no. 4, 2002.
[10] Kugelstadt, T., *Op Amps for Everyone: Chapter 16 - Active Filter Design Techniques.* Texas Instruments.
[11] Binette, J. S. *et al.*, *Tetrapolar Measurement of Electrical Conductivity and Thickness of Articular Cartilage.* Journal of Biomechanical Engineering, vol. 126, pp. 475 - 484, 2004.
[12] Laufer, S. *et al.*, *Electrical impedance characterization of normal and cancerous human hepatic tissue.* Physiological Measurement, vol. 31, pp. 995 - 1009, 2010.